Tuijin Jishu/Journal of Propulsion Technology
ISSN: 1001-4055
Vol. 45 No.1 (2024)

Smart Farming Solutions: An Integrated Approach to Agro-Product Quality Assessment using Thermal Imaging and Machine Learning

Zeeshan ali Haq[1], Zainul Abdin Jaffery[2], Shabana Mehfuz[2]

[1] *Dept of Computer Science & Engineering, SEST, Jamia Hamdard, New Delhi, India*

[2] *Dept of Electrical Engineering, FET, Jamia Millia Islamia, New Delhi, India*

Abstract: Classification of Potatoes into Defective and non-defective is an important area of impact for agriculture based industries. In this paper, quality of agro-products are assessed to aid in the development of neural network and thermal imaging based automated computer vision system. For classification, object features are extracted from thermally generated images. The primary dataset of 480 thermally generated images is developed. Various colour and statistical based features are used as an input to the neural network. Two hidden layers based Artificial Neural Network (ANN) based models are used. Impact of each feature is determined by considering a single-input ANN. Multi-input ANN based models are deployed to assess the performance of each features in combination with other features. Entropy and Energy provides high classification accuracy. Variance is observed to be a poor feature for classification. Considering all the features, except variance, 98.4% of classification accuracy is achieved.

Keywords: *Agriculture Products, Artificial Neural Network, Feature Extraction, Image Processing, Thermal Imaging*

1. Introduction:

Quality of vegetables and fruits are assessed based on its nutrient content, shape, degree of ripeness, etc. Industries based on processing of Agro-products require high quality food materials to increase their productivity and profit margin. Agro-products are segregated into good or bad based on quality assessment process. The characteristics of poor quality products vary from different types of disease, bruises, deformation, its nutrient content, size and texture of the products. In early days, segregation of agro-products were based on human identification of these characteristics. This manual process has its own limitations. The manual system is exhaustive, time consuming and tiring. This leads to increase in error in detection and farm to market time. Many researchers are working to develop an automated systems that reduces human interference, thus reducing the time and physical labor considerably.

With the evolution of computer-based technologies and tools, it has become imperative to use them in the development of automated systems for classification and defect detection. In recent years, various imaging methods based on spectrums are being used for the detection of defects in agricultural products. Some of the spectrums that are being explored includes visible, infrared, near infrared and Hyperspectral.

Pholpho et al, Wu et al, Jimenez-Jimenez et al, and Luo et al, [1-4] have used visible frequency imaging system for the quality analysis of the agro-product. However, their work is limited to detecting single defect in the fruits. In other research, same kind of camera is applied to analyze multiple types of defects in citrus fruits [5]. Other researchers employ Hyperspectral Imaging (HSI) System for defect or bruise detection. Work done for

classification and defect detection in apples [6-8] using classification models such as LDA, SVM, Neural Networks has been performed. Other work including defect detection in agro-products using HSI system includes detection of microbial infection in oranges and bruise and skin defects in pears [9-11]

In terms of accuracy and other classification parameters, both of these imaging techniques performed well. However, these imaging techniques have certain drawbacks. Visible Spectrum imaging technique is not suitable for poorly illuminated or dark colored objects. Hyperspectral imaging systems, on the other hand, may necessitate a significantly large computational time and large storage space, which is not advisable for real-time embedded systems. Recently infrared thermal imaging based techniques are gaining popularity for quality assessment in various industries [12-14]. Thermal image is the temperature profile of the object under consideration. It is also a century old fact that temperature is the major parameter that give health condition of an object. Thermal imaging is based on the Stefan Bolzman equation which describes the relationship between an object's temperature and the radiation generated by a unit area of that object. It is a non-invasive and non-contact method, thus it can be easily used in the areas difficult to reach. It is also best suited for the objects that may be contaminated by touching. This technique is not light-dependent and can be used on dark-colored agro-products and is computationally more efficient than HSI technique.

Many researchers have studied statistical and neural network-based methods for defect detection and Classification. Kuzy et. al. and Doosti-Irani et. al. have used statistical methods such as Analysis of Variance (ANOVA), Multivariate Analysis of Variance (MANOVA), Pearson Correlation Analysis (PCA), and Multiple Regression Model for defect detection and classification in blueberries and apples respectively [15-16]. Kim et al employ the Lock-in Thermography method to optimize bruise detection in pears [17]. Baranowski et al implemented the Hyperspectral and pulse-phase thermal imaging to detect early bruises in apples [18]. For differentiation between healthy and non-healthy tissues of apples, they used Principle Component Analysis (PCA) and MNF. For result validation Linear Discriminant Analysis (LDA), Support Vector Machine (SVM) and Minimum Noise Function (MNF). Varith et al employed thermal imaging system to detect apple bruises [19]. The author processed the apples using a heating and cooling system, observing the before and after thermal images of the apples, checking for bruises due to temperature variation, and studying the temperature decay over time. Jiao et al administered a thermal imaging technique to monitor the deterioration of peach fruit in an uncertain environment [20]. Over the course of 56 hours, six different time-varying thermal images were captured. The temperature decay of the bruised surface were used to evaluate peach bruising.

Researchers have used different types of Deep Learning Neural Networks for the classification of fruits and vegetables using standard classification algorithms such as LDA, SVM, Decision Tree, Random Forest, K-Nearest Neighbor, and Artificial Neural Networks. Kavdir et al used textural features to classify apples using ANN and statistical analytical tools [21]. Zheng et al employed a pre-trained CNN training model, LeNet, on a dataset of 4371 thermal images from 300 harvested pears to classify bruises [22].

Deep Learning Neural Networks for the classification in agro-product is also being practiced. Many researcher have implemented the standard classification algorithms such as LDA, SVM, Decision Tree, Random Forest, K-Nearest Neighbor, etc for training the network for fruits defect detection and classifications. It is an effective classification model but is computationally expensive which necessitates a large database in order to achieve higher classification accuracy. ANN, on the other hand, require a smaller database. The application of image processing in combination with neural network-based classification algorithms has improved the effectiveness of automated agro-product defect detection systems.

In this paper, thermal images are used in conjunction with an ANN based classification model for classification of defective and non-defective potatoes. Thermal images are captured using a FLUKE TiS45 and database is created. These images are converted into an equivalent grayscale images from which seven first-order-histogram based features are extracted. These features are accepted as an input to the ANN model for defective and non-defective potato classification. Performance of individual and combination of features are evaluated and their results are presented. The proposed model for combination of six features provides the highest classification accuracy of 94.89%. The flow of the paper is as follows: section II describes a detailed methodology for dataset

generation, defect detection and classification, and performance evaluation parameters. The simulation output for each step of the proposed methodology is presented in Section III and Section IV provides a complete simulation result of the proposed model. The paper is concluded in section V.

2. Material & Methodology

2.1 Hardware and Software

Thermal camera captures the infrared radiation of an object and generates an equivalent image as a function of temperature. Thermal image of potato is captured by TiS45, a thermal imager by Fluke Corporation, USA. The imager has the operating frequency of -10ºC to +50ºC, spectral range of 7.5µm to 14µm, and focal plane array of 160x120 pixels. The ambient temperature while capturing the thermal images of potato is in the range of 30ºC to 35ºC and standard emissivity value of 0.95. The proposed model is simulated done using Python on Google Colab Pro with 32GB of main memory, Nvidia A100 GPU with 16GB of GPU RAM and Intel Xeon CPU (subjective to availability). Figure 1 shows a flow diagram of the proposed methodology

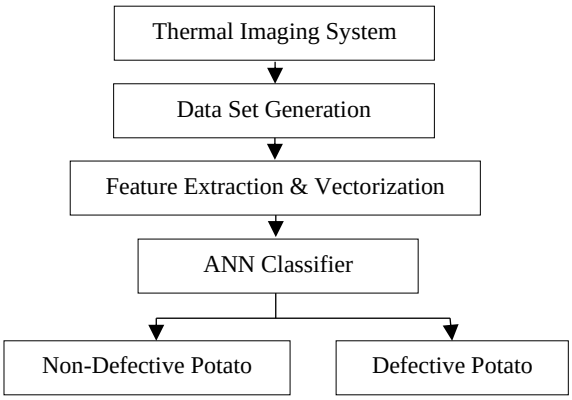

Figure 1: Flow diagram of Proposed Methodology

2.2 Thermal Imaging System

Thermal images of defective and non-defective potatoes are captured using a thermal imaging system (figure 2). To maintain the temperature of the object, pulse phase thermographic method is employed where a constant stream of hot air is administered to the object. The decay in the infrared waves produced by the object are captured by thermal imager and saved on the processing system. A constant distance between the object and the camera of 15cm is maintained.

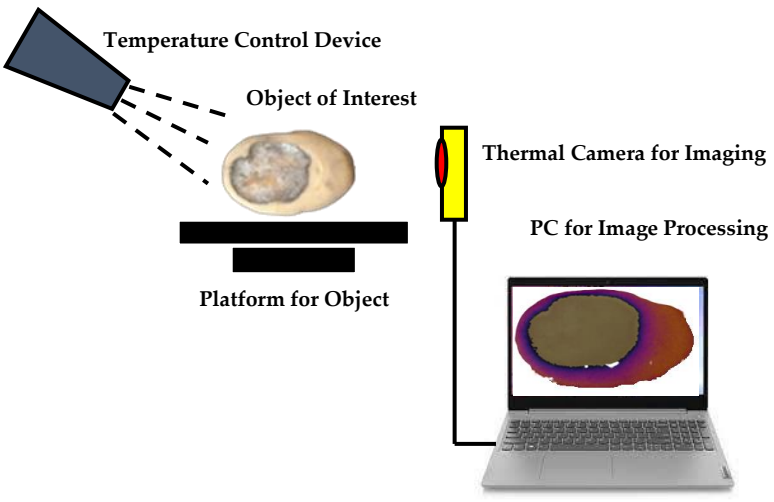

Figure 2: Thermal Imaging System

2.3 Dataset Development

Thermal images of potato are captured using the imaging system as shown in figure 2. These images are stored to develop the dataset for the neural network base model. A sample of thermal images for defective and non-defective potatoes are shown in figure 3. In this study, the size of the complete dataset is 480 thermal images of which 250 image belongs to the defective class and 230 image belongs to the non-defective class. The dataset is divided into two parts: training and testing. The testing dataset of 80 images (41 defective class and 39 non-defective class) is kept hidden during the training phase. The training dataset consist of 400 thermal images including 209 images for defective class and 191 images for non-defective class. A validation set consisting of 160 randomly selected images, from the training dataset, including 84 images for defective class of potato and 76 images for non-defective class of potato is considered at each iteration of the model.

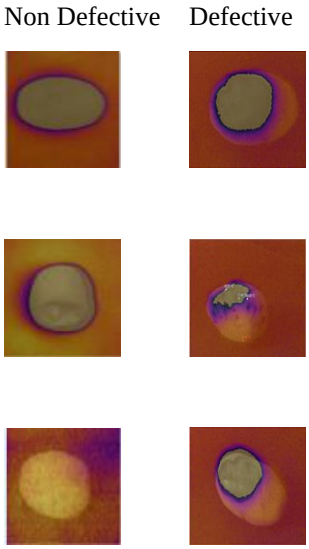

Figure 3 Sample of Data Generated for different classes

2.4 Feature Extraction

Thermal images stored in the dataset, figure 3, are in RGB channel. These images are converted to the grayscale images to reduce the dimensionality of the dataset. First order histogram based and statistical based features are extracted from the grayscale images. Seven feature are considered in this study including Kurtosis, Skewness, Variance, Standard Deviation, Mean, Entropy, and Energy. These extracted features from each images are stored in an array to be considered as an input for the neural network model used for classification. These features are presented in table 1.

Table 1: List of Features

Feature Type	Feature Name	Abbreviation
Higher Order histogram based feature	Kurtosis	K
	Skewness	S
Lower Order Statistical based feature	Mean	M
	Variance	V
	Standard Deviation	SD
Higher Order Statistical based feature	Shannon Entropy	SE

	Energy	E

2.5 Development of ANN classifier

In this paper Artificial Neural Network based model for classification of potatoes into two classes: Non-defective and defective is developed. The motivation towards employing the traditional ANN model includes the computational efficiency, faster classification, and easy deployment. In this paper Multi-layer Perceptron (MLP) based algorithm is used as the architecture for neural network. The ANN model has three sets of layers: input layer, hidden layers, and the output layer as shown in figure 4. The number of neurons deployed in the input layer are variable in nature and depends on the number of features being considered. The output layer consists of two neurons and Softmax activation function [23].

Two hidden layers are implemented with 500 and 200 neurons respectively, each with ReLu activation function. Number of neurons in the hidden layer are adjusted using the 'Dropout' functionality of the simulation which optimizes the number of neurons. The final relationship between input and output layer is determined by the adjustment of the weights connecting neurons. The adjustment of weights connecting the neurons are performed iteratively using backward and forward propagation. Backward propagation updates the weights and forward propagation calculates the error based on accuracy and loss due to those weights. This adaptive nature of the network provides an optimized model for classification. The features used as the variables to the input layers is propagated through the network and by the action of weight and activation function on these features, the network is able to classify the potato into different classes.

In the proposed model, on close examination, it is observed that with a learning rate of 0.001, the network is optimized. For backward propagation method, Adam optimizer is considered which is similar to the gradient descent algorithm but instead of applying the gradient on the function of the targeted point directly, Adam optimizer uses the gradient of function to calculate the first and second moment of the targeted value. These moments are used to update the weight of the neurons. The network model is iterated for 30 epochs.

$$\boldsymbol{\omega(t) = \omega(t-i) - \alpha \frac{\hat{m}(t)}{\sqrt{\hat{v}(t)+\epsilon}};} \quad \mathbf{1 \le i \le k} \tag{1}$$

Where, $\boldsymbol{\omega(t)}$ is the updated weight value, $\boldsymbol{i}$ = number of epochs, $\boldsymbol{k}$ = maximum number of epochs, $\boldsymbol{\alpha}$ is the learning rate, $\boldsymbol{\hat{m}(t)}$ is the bias corrected value of first moment (mean), $\boldsymbol{\hat{v}(t)}$ is the bias corrected value of the second moment (variance), and $\boldsymbol{\epsilon}$ is the parameter to avoid the zero division problem and its value is kept typically very small. For calculation of error between predicted and actual value of the data in terms of accuracy and loss forward propagation is used following the mathematical equation 2

$$\boldsymbol{y_i = \rho(b_i + x_i * \omega_i)} \tag{2}$$

Where, $\boldsymbol{y_i}$ is the neuron output, $\boldsymbol{\rho}$ is the activation function of the neuron, $\boldsymbol{b_i}$ is the bias for initializing the neuron, and $\boldsymbol{x_i}$ is the input to the current layer of the hidden layer which is also the output from the previous layer. Binary cross entropy is used as a loss function which compares the actual and predicted values

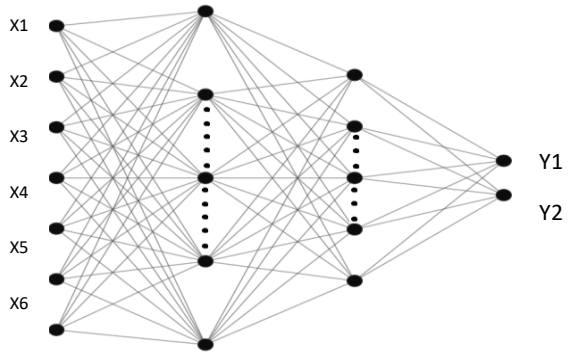

Figure 4: Neural Network

2.6 Performance Evaluation parameters

To evaluate the performance of the proposed system following parameters are evaluated and compared to determine the optimum performance model for classification.

Accuracy (A): It is the ratio of total no of data classified correctly to the total no of data in the data set. Mathematically it is given by equation

$$A = \frac{Total\ no\ of\ correct\ assessment}{total\ no\ of\ all\ assessment} = \frac{TN + TP}{Total\ Predictions} \quad (3)$$

Precision (P): It is the positive predicted value. It evaluates the degree of positive classification which are actually positive.

$$P = \frac{TP}{TP + FP} \quad (4)$$

Recall (R): It gives ratio of total positive predicted data to the total actual positive data. It is also called as Sensitivity

$$R = \frac{TP}{TP + FN} \quad (5)$$

F-1 Score is the higher order combinatorial matrix of precision and recall.

$$F - 1\ Score = 2 * \left(\frac{P * R}{P + R}\right) \quad (6)$$

Where;

TP (True Positive): data is actually positive and is also predicted as positive.

TN (True Negative): data is actually negative and is also predicted as negative.

FP (False Positive): data is actually negative but is predicted as positive

FN (False Negative): data is actually positive but is predicted as negative.

Using the above description of TP, TN, FP, and FN a confusion matrix is generated as shown in figure 5.

		Predicted	
		Non-Defective	**Defective**
Observed	**Non-Defective**	True Positive	False Negative
	Defective	False Positive	True Negative

Figure 5: Confusion matrix

3. Simulation Result

The proposed model for classification of potatoes is performed for one sample from each class and their respective results are presented in this section. For the sample simulation of the model, all seven features are considered. The algorithm for simulation of the developed model is shown in figure 6. This algorithm consist of two parts. The first part is for feature extraction and generating a vectored array of feature. The second part uses this feature array as an input to the classification model.

Input → corpus of Images to be classified

Output → Prediction

Corpus = Set of all thermal images

for *image* **in** *corpus* **do**

gray_img = rgb_to_gray(image)

K = kurtosis(gray_img)

S = skewness(gray_img)

M = mean(gray_img)

V = variance(gray_img)

SD = standard_deviation(gray_img)

SE = Shanon_entropy(gray_img)

E = energy(gray_img)

Feat = [K,S,M,V,SD,SE,E]

Img_features = Img_features.append(*Feat*)

end

Scaled_features = Min_Max_Scaling(Img_features)

For *features* **in** *Scaled_features* **do**

Model = load_ANN_Model

Prediction = ANN_Model(Feature)

end

Figure 6: algorithm for proposed model

Step 2 of the model converts the thermally images of the dataset into the equivalent grayscale images. All the features are extracted from these grayscale images, and stored in a single array in step 3. Since the values for these features are heavily skewed, feature scaling is administered to normalize the values in step 4. This is important to involve equal participation of each feature in classification process. These features are propagated through the model, and using forward and backward propagation methods, the weight optimization is achieved. Finally, in step 5, the output is obtained in terms of probability for classifying the object into either class. Based on the probability achieved in step 5, the potatoes are classified into either defective or non-defective class.

Table 2: step wise result of proposed methodology

Steps	**Non-defective Potato**	**Defective Potato**
Step 1: Captured Image	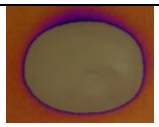	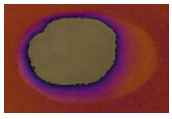
Step 2: Gray Scale image	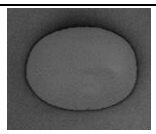	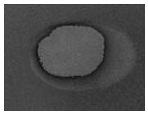
Step 3: Features of Image	K 5.98840351 S -1.76220199	K 2.023527 S -1.4894787

	M 11.59286264 SD 81.5141566 SE 4.38183408 E 5.53889269	M 18.00129207 SD 83.53689846 SE 5.74982747 E 2.81695787
Step 4: Features Scaling	K -0.58828428 S -1.56893667 M -1.48091018 SD -0.08037347 SE -0.82732362 E -0.70364438	K -0.83755939 S -1.42365514 M -0.09562881 SD 0.14799461 SE 1.09261631 E -0.85029113
Step 5: classification Probability	$\begin{bmatrix}0.9929617\\0.00703825\end{bmatrix} = \begin{bmatrix}1\\0\end{bmatrix}$	$\begin{bmatrix}0.00001513\\99.9984860\end{bmatrix} = \begin{bmatrix}0\\1\end{bmatrix}$
Step 6: Classification	**Non-defective Potato**	**Defective Potato**

The classification model performance is evaluated in two phase. During the first phase, each feature is considered individually and the performance of the model is evaluated based on accuracy and classification report. During the second phase of the simulation of the classification model, the combination of features are used to determine the accuracy of the model

4 Result & Discussion

A step-by-step simulation of two sample of thermal images from the dataset is discussed in the previous section. In this section the proposed model of classification is implemented over the entire dataset. Performance of the model of single feature and combination of features are presented and evaluated based on different performance evaluation metrics.

4.1 System Performance for individual features

The classification model, during the first phase of implementation, is a single-input ANN model where each feature is considered as an input individually. For each feature, the model is iterated for 30 epochs. The input is propagated through the model network and classification of potato is performed. Table 3 presents the accuracy of the single-input classification model when each feature is considered individually. From the table it is observed that Entropy and Energy feature performs best while considering the classification based on thermal images considering the histogram and statistical based features. Considering the Entropy feature, a high validation accuracy of 82.49% is achieved and for Energy feature 81.27% of testing accuracy is achieved. From the table, it is also observed that Variance does not performs as well as the other features giving only 53.28% of testing accuracy.

Table 3: Individual Feature Performance

Feature	**Accuracy (%)**		
	Training	**Validation**	**Testing**
Kurtosis	67.5	60	58.23

Skewness	75	77.49	78.13
Variance	52.49	50	53.28
Mean	69.37	62.5	64.53
Standard Deviation	66.25	72.5	70.82
Entropy	**76.87**	**82.49**	79.81
Energy	71.24	80.38	**81.27**

Other performance evaluation parameters included in the classification report such as Precision, Recall, and F-1 Score are presented in Table 4 for single-input classification model. As presented in table 4, it is observed that for the classification report parameters, the feature of Entropy, Energy, and Standard Deviation have higher values. As presented in table 3, it is again confirmed from these parameters that variance is not a very good feature for thermal image based classification.

Table 4: Class wise classification report for each feature considered individually

Feature	**Class wise classification report**					
	Precision		**Recall**		**F-1 Score**	
	NDP	**DP**	**NDP**	**DP**	**NDP**	**DP**
Kurtosis	0.9	0.55	0.29	0.95	0.43	0.69
Skewness	**1**	0.7	0.62	**1**	0.76	0.83
Variance	0.8	0.5	0.44	**1**	0.55	0.67
Mean	**1**	0.56	0.29	**1**	0.44	0.72
Standard Deviation	0.8	0.65	0.75	0.69	0.77	0.67
Entropy	**1**	0.76	0.61	**1**	0.76	**0.86**
Energy	0.8	**0.89**	**0.89**	0.76	**0.83**	0.82

4.2 System Performance for Combination of feature

In this section, the performance of multi-input classification model is presented. For each model simulation, a feature is added to the previous set of features used in previous model simulation. The model performance based on accuracy and classification report is presented in table 5 and table 6 respectively. Theoretically it is understood that as the number of features are increased, the classification performance of Neural Network is improved. The same conclusion is achieved here also by adding each feature, the performance of the classification model is improved. As shown in table 5, classification accuracy of 91.26% and 87.29% is achieved for ε and λ. From the previous section, it is observed from table 3 and table 4, that variance performs poorly as an input to the network. Therefore, for 'τ' set of features, accuracy of 94.89% is achieved. Also this set of features has only 8% of loss during classification.

Feature	**Abbreviation**	**Data set**	**Accuracy (%)**	**Training Loss**
K+S	α	Training	74.37	0.45
		Validation	82.49	

		Testing	79.65	
K+S+V	β	Training	72.5	0.51
		Validation	57.49	
		Testing	61.34	
K+S+V+M	γ	Training	85	0.34
		Validation	87.5	
		Testing	88.4	
K+S+V+M+SD	δ	Training	92.5	0.18
		Validation	87.5	
		Testing	84.38	
K+S+V+M+SD+SE	ε	Training	83.74	0.38
		Validation	89.99	
		Testing	91.26	
K+S+V+M+SD+SE+E	λ	Training	84.37	0.37
		Validation	89.99	
		Testing	87.29	
K+S+M+SD+SE+E	τ	Training	97.5	0.08
		Validation	95.99	
		Testing	**94.89**	

The variation of accuracy and loss of the model with respect to number of epochs for different set of features is shown graphically in figure 7. In these figures also it can be seen that the curve representing six features excluding variance feature is providing the best performance by the model.

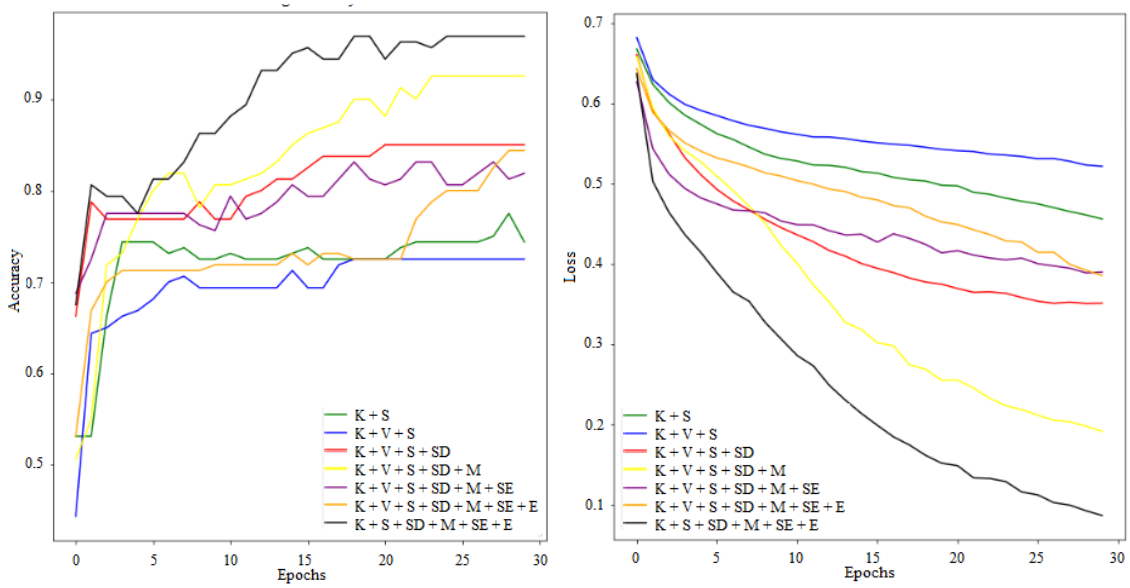

Figure 7: Performance Evaluation Curve (a) curve between no of epochs and Accuracy of the model (b) curve between no of epochs and the testing loss of the model.

A class wise classification report for the proposed model for different set of configurations is presented in table 6. Here also it is observed that, with higher number of features, the classification report improves. Also, with removal of variance as a feature, the performance of the model improves. This also elevates the fact that for this type of classification, variance is not a good feature to be considered

Table 6: class wise classification report for combination of Features

Combination of Features	Precision	Recall	F-1 Score	Class
K+S	0.88	0.74	0.80	DP
	0.79	0.90	0.84	NDP
K+S+V	0.52	0.83	0.64	DP
	0.73	0.36	0.48	NDP
K+S+V+SD	0.83	0.98	0.91	DP
	1.00	0.67	0.80	NDP
K+S+V+SD+M	0.92	0.88	0.90	DP
	0.81	0.87	0.84	NDP
K+S+V+SD+M+SE	0.84	0.97	0.91	DP
	1.00	0.79	0.88	NDP
K+S+V+SD+M+SE+E	0.84	0.94	0.89	DP
	0.95	0.87	0.91	NDP
K+S+SD+M+SE+E	0.92	0.98	0.96	DP
	1.00	0.88	0.94	NDP

In this study it is observed that combination of six first-order histogram and statistical based feature performs better than other combinations. A confusion matrix for the same set of six features is shown in figure 8. As discussed in previous section, the testing dataset consist of 80 thermally generated images of defective and non-defective potatoes. Using the combination of six features, 38 images of non-defective potatoes out of 39 images are positively classified as non-defective and 39 images of defective potatoes out of 41 images are positively classified as defective potatoes.

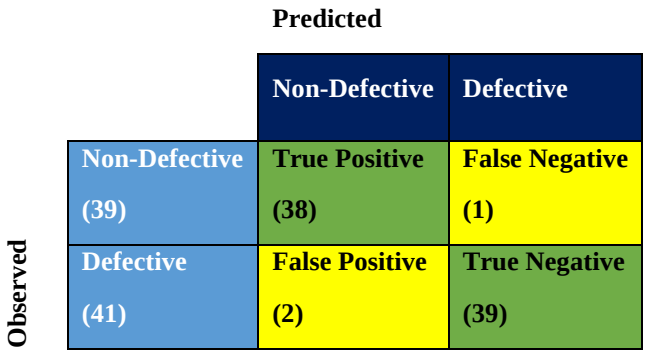

Figure 8: Confusion Matrix for segregation of defective and non-defective potatoes

5 Conclusion

In this paper, an algorithm is developed for classification of defective and non-defective potatoes using thermal imaging and neural network. Feature extraction technique is implemented to optimize the classification model. Total of 480 thermal images of potatoes are captured using the thermal imaging system of which 250 belong to the defective class and 230 belong to the non-defective class. For this study, seven first-order-histogram and statistical based features are considered. These features are extracted from the grayscale converted thermally generated images from defective and non-defective potatoes. The model development is carried in two phase. The first phase consist of single-input classification model and the second phase consist of the multi-input classification model. During the first phase it is observed that Entropy and Energy are the best feature for thermal image classification whereas Variance feature performs poorly. During the second phase, the same observation is utilized and highest classification accuracy is achieved when Variance feature is excluded from the set of all the features. Considering this set of features (τ), classification accuracy of 97.5% is achieved. Also, the other parameter for performance evaluation, the classification report including Precision, Recall, and F-1 Score has highest value among all the set of features.

References

[1] Pholpho, T., S. Pathaveerat, and P. Sirisomboon. 2011. Classification of longan fruit bruising using visible spectroscopy. Journal of Food Engineering 104 (1):169–72. doi: 10.1016/j.jfoodeng.2010.12.011.

[2] Wu, G. F., and C. G. Wang. 2014. Investigating the effects of simulated transport vibration on tomato tissue damage based on vis/nir spectroscopy. Postharvest Biology and Technology 98:41–7. doi: 10. 1016/j.postharvbio.2014.06.016

[3] Jimenez-Jimenez, F., S. Castro-Garcia, G. L. Blanco-Roldan, J. AgueraVega, and J. A. Gil-Ribes. 2012. Non-destructive determination of impact bruising on table olives using vis-nir spectroscopy. Biosystems Engineering 113 (4):371–8. doi: 10.1016/j.biosystemseng. 2012.09.007.

[4] Luo, X., T. Takahashi, K. Kyo, and S. Zhang. 2012. Wavelength selection in vis/nir spectra for detection of bruises on apples by roc analysis. Journal of Food Engineering 109 (3):457–66. doi: 10.1016/j.jfoodeng.2011.10.035.

[5] Zhang, W., Z. Z. Lv, and S. L. Xiong. 2018. Nondestructive quality evaluation of agro-products using acoustic vibration methods-A review. Critical Reviews in Food Science and Nutrition 58 (14): 2386–97. doi: 10.1080/10408398.2017.1324830

[6] Baranowski, P., W. Mazurek, and J. Pastuszka-Wozniak. 2013. Supervised classification of bruised apples with respect to the time after bruising on the basis of hyperspectral imaging data. Postharvest Biology and Technology 86:249–58. doi: 10.1016/j.postharvbio.2013.07.005.

[7] Baranowski, P., W. Mazurek, J. Wozniak, and U. Majewska. 2012. Detection of early bruises in apples using hyperspectral data and thermal imaging. Journal of Food Engineering 110 (3):345–55. doi: 10.1016/j.jfoodeng.2011.12.038.

[8] Huang, W., B. Zhang, J. Li, and C. Zhang. 2013. Early detection of bruises on apples using near-infrared hyperspectral image. In Piageng 2013: Image processing and photonics for agricultural engineering, eds H. Tan, 8761. Bellingham: Spie-Int Soc Optical Engineering. doi:10.1117/12.2019630

[9] Yin, S., X. Bi, Y. Niu, X. Gu, and Y. Xiao. 2017. Hyperspectral classification for identifying decayed oranges infected by fungi. Emirates Journal of Food and Agriculture 29 (8):601–9. doi: 10.9755/ejfa.2017-05-1074.

[10] Li, J. B., R. Y. Zhang, J. B. Li, Z. L. Wang, H. L. Zhang, B. S. Zhan, and Y. L. Jiang. 2019. Detection of early decayed oranges based on multispectral principal component image combining both bi-dimensional empirical mode decomposition and watershed segmentation method. Postharvest Biology and Technology 158:110986. doi: 10.1016/j.postharvbio.2019.110986

[11] Lee, W.-H., M. S. Kim, H. Lee, S. R. Delwiche, H. Bae, D.-Y. Kim, and B. K. Cho. 2014. Hyperspectral near-infrared imaging for the detection of physical damages of pear. Journal of Food Engineering 130:1–7. doi: 10.1016/j.jfoodeng.2013.12.032

[12] Jaffery, Zainul Abdin. "Thermal image based Monitoring of PV modules and Solar Inverters." Reliability of Power Electronics Converters for Solar Photovoltaic Applications (2021): 189.
[13] Singh, Laxman, et al. "Design of thermal imaging-based health condition monitoring and early fault detection technique for porcelain insulators using Machine learning." Environmental Technology & Innovation 24 (2021): 102000.
[14] N. Sabah and Z. A. Jaffery, "Fault Detection of Induction Motor Using Thermal Imaging," 2022 IEEE IAS Global Conference on Emerging Technologies (GlobConET), Arad, Romania, 2022, pp. 84-90, doi: 10.1109/GlobConET53749.2022.9872516.
[15] Kuzy, Jesse, Yu Jiang, and Changying Li. "Blueberry bruise detection by pulsed thermographic imaging." Postharvest Biology and Technology 136 (2018): 166-177.
[16] Doosti-Irani, Omid, et al. "Development of multiple regression model to estimate the apple's bruise depth using thermal maps." Postharvest Biology and Technology 116 (2016): 75-79.
[17] Kim, Ghiseok, et al. "Application of infrared lock-in thermography for the quantitative evaluation of bruises on pears." Infrared Physics & Technology 63 (2014): 133-139.
[18] Baranowski, Piotr, et al. "Detection of early bruises in apples using hyperspectral data and thermal imaging." Journal of Food Engineering 110.3 (2012): 345-355.
[19] Varith, J., et al. "Non-contact bruise detection in apples by thermal imaging." Innovative Food Science & Emerging Technologies 4.2 (2003): 211-218.
[20] Jiao, L. Z., et al. "The infrared thermal image-based monitoring process of peach decay under uncontrolled temperature conditions." Journal of Animal and Plant Sciences 3.1 (2015): 202-207.
[21] Kavdır, I., and D. E. Guyer. "Comparison of artificial neural networks and statistical classifiers in apple sorting using textural features." Biosystems Engineering 89.3 (2004): 331-344.
[22] Zeng, Xiangyu, et al. "Detection and classification of bruises of pears based on thermal images." Postharvest Biology and Technology 161 (2020): 111090.
[23] Z. A. Haq and Z. A. Jaffery, "Impact of Activation Functions and Number of Layers on the Classification of Fruits using CNN," 2021 8th International Conference on Computing for Sustainable Global Development (INDIACom), New Delhi, India, 2021, pp. 227-231.